Expected nuclear modifications and pseudorapidity asymmetry in p(d)Pb collisions at the LHC

Adeola Adeluyi
Center for Nuclear Research
Department of Physics
Kent State University, USA
E-mail: `aadeluy1@kent.edu`

Gergely G. Barnaföldi
Center for Nuclear Research
Department of Physics
Kent State University, USA
E-mail: `bgergely@rmki.kfki.hu`

George Fai[*]
Center for Nuclear Research
Department of Physics
Kent State University, USA
E-mail: `gfai@kent.edu`

Péter Lévai
MTA KFKI RMKI Research Institute for Particle and Nuclear Physics
P.O. Box 49, Budapest 1525, Hungary
E-mail: `plevai@rmki.kfki.hu`

We calculate nuclear modification factors and pseudorapidity asymmetries in *pA* and *dA* collisions in a pQCD-improved parton model. With the calculations tuned to describe existing spectra from *pp* collisions and asymmetric systems at midrapidity and large rapidities at FNAL and RHIC energies, we make predictions for LHC energies.

High-pT Physics at LHC - Tokaj'08
March 16 - 19 2008
Tokaj, Hungary

[*]Speaker.

1. Introduction

Asymmetric systems offer unique information about the underlying dynamics, not available in symmetric proton-proton or nucleus-nucleus collisions. The asymmetry manifests itself in an asymmetric distribution of charged particles with respect to zero rapidity (or pseudorapidity) as measured by BRAHMS [1] and PHOBOS [2]. The asymmetry can be quantified by introducing the ratio of pseudorapidity densities at a given negative pseudorapidity relative to that at the positive pseudorapidity of the same magnitude. This backward/forward ratio (forward being the original direction of motion of the light partner) is referred to as pseudorapidity asymmetry. The STAR Collaboration published pseudorapidity asymmetries in 200 *AGeV dAu* collisions for several identified hadron species and total charged hadrons in the pseudorapidity intervals $|\eta| \leq 0.5$ and $0.5 \leq |\eta| \leq 1.0$ [3]. Asymmetries with the backward/forward ratio above unity for transverse momenta up to ≈ 5 GeV/c are observed for charged pion, proton+anti-proton, and total charged hadron production in both rapidity regions. We anticipate that proton-lead (or deuteron-lead) data will soon be collected at higher energies, at the Large Hadron Collider (LHC).

In the present study we investigate the roles of nuclear shadowing and multiple scattering in the generation of nuclear modifications and pseudorapidity asymmetries in a wide transverse-momentum range. We use the HIJING shadowing parameterization [4] and the Eskola–Paukkunen–Salgado (EPS08) nuclear parton distribution functions (nPDFs) [5]. While the former has been applied widely, the latter was not available at the time of similar earlier studies. We present pseudorapidity asymmetries for *pBe* at 30.7 GeV (Fermilab) and *dAu* at 200 *A*GeV (RHIC), where data are available from the E706 experiment [6], PHENIX [7], and STAR [3]. We then make predictions for *dPb* at 8.8 *A*TeV (LHC).

2. Model framework

The invariant cross section for the production of final hadron *h* from the collision of nucleus *A* and nucleus *B* ($A + B \rightarrow h + X$), can be written as

$$E_h \frac{\mathrm{d}^3 \sigma_{AB}^h}{\mathrm{d}^3 p} = \sum_{abcd} \int \mathrm{d}^2 b \, \mathrm{d}^2 r \, t_A(b) t_B(|\vec{b} - \vec{r}|) \mathrm{d}x_a \mathrm{d}x_b \mathrm{d}\vec{k}_{Ta} \mathrm{d}\vec{k}_{Tb} \, \mathrm{d}z_c \, f_{a/A}(x_a, \vec{k}_{Ta}, Q^2)$$

$$f_{b/B}(x_b, \vec{k}_{Tb}, Q^2) \frac{\mathrm{d}\sigma(ab \rightarrow cd)}{\mathrm{d}\hat{t}} \frac{D_{h/c}(z_c, Q_f^2)}{\pi z_c^2} \hat{s} \delta(\hat{s} + \hat{t} + \hat{u}) , \qquad (2.1)$$

where all quantities have their usual meaning [8].

The collinear parton distribution functions (PDFs) are generalized to include a transverse momentum degree of freedom, $\vec{k}_T$, as required by the uncertainty principle. This can be formally implemented in terms of unintegrated PDFs [9, 10]. To avoid some of the complications associated with using unintegrated PDFs, we resort to a simple factorized approximation, where the k_T-broadened parton distribution in the nucleon is written as

$$f_{a/N}(x, \vec{k}_T, Q^2) \longrightarrow g(\vec{k}_T) \cdot f_{a/N}(x, Q^2), \quad g(\vec{k}_T) = \frac{\exp(-k_T^2 / \langle k_T^2 \rangle_{pp})}{\pi \langle k_T^2 \rangle_{pp}} , \qquad (2.2)$$

where $f_{a/N}(x, Q^2)$ is the standard collinear PDF in the nucleon, and $\langle k_T^2 \rangle_{pp}$ is the two-dimensional width of the transverse-momentum distribution in the proton, related to the magnitude of the average transverse momentum of a parton by $\langle k_T^2 \rangle_{pp} = 4\langle k_T \rangle_{pp}^2 / \pi$.

Most shadowing parameterizations include at least some of the effects of multiple scattering in the nuclear medium, while the HIJING parameterization needs to be augmented with modeling nuclear multiscattering [8]. For this purpose, in *pA* collisions we use a broadening of the width of the transverse momentum distribution according to

$$\langle k_T^2 \rangle_{pA} = \langle k_T^2 \rangle_{pp} + C \, h_{pA}(b) \,, \tag{2.3}$$

where $\langle k_T^2 \rangle_{pp}$ is the width already present in proton-proton collisions, $h_{pA}(b)$ is the number of effective nucleon-nucleon (*NN*) collisions as a function of nucleon impact parameter *b*, and *C* is the average increase in width per *NN* collision.

The collinear nPDFs $f_{a/A}(x, Q^2)$ are expressible as convolutions of nucleonic parton distribution functions (PDFs) $f_{a/N}(x, Q^2)$ and a shadowing function $S_{a/A}(x, Q^2)$ which encodes the nuclear modifications of parton distributions. We use the MRST2001 next-to-leading order (NLO) PDFs [11] for the nucleon parton distributions and for the shadowing function we employ both HIJING [4] and EPS08 shadowing routine [5]. (Other nPDFs, like FGS [12], HKN [13], and the earlier EKS [14], are used elsewhere to calculate pseudorapidity asymmetries [15].) For the final hadron fragmentation we utilize the fragmentation functions in the AKK set [16]. The factorization and fragmentation scales are from the best-fit results obtained in Ref. [17]. We obtain the density distribution of the deuteron from the Hulthen wave function [18] (as in Ref. [19]), while a Woods-Saxon density distribution is used for gold and lead with parameters from Ref. [20].

3. Nuclear modifications and pseudorapidity asymmetry

The nuclear modification factor, $R_{AB}^h(p_T, \eta)$, and pseudorapidity asymmetry, $Y_{Asym}(p_T)$, can be defined for any produced hadron species *h* as

$$R_{AB}^h(p_T, \eta) = \frac{1}{\langle N_{bin} \rangle} \cdot \frac{E_h \mathrm{d}^3 \sigma_{AB}^h / \mathrm{d}^3 p|_\eta}{E_h \mathrm{d}^3 \sigma_{pp}^h / \mathrm{d}^3 p|_\eta}, \quad Y_{Asym}^h(p_T) = E_h \frac{\mathrm{d}^3 \sigma_{AB}^h}{\mathrm{d}^3 p}\bigg|_{-\eta} \bigg/ E_h \frac{\mathrm{d}^3 \sigma_{AB}^h}{\mathrm{d}^3 p}\bigg|_\eta \,, \tag{3.1}$$

where $\langle N_{bin} \rangle$ is the average number of binary nucleon-nucleon collisions.

Let us consider the (double) ratio of the forward and backward nuclear modification factors in *dAu* collisions for species *h*:

$$R_\eta^h(p_T) = \frac{R_{dAu}^h(p_T, -\eta)}{R_{dAu}^h(p_T, \eta)} = \frac{E_h \mathrm{d}^3 \sigma_{dAu}^h / \mathrm{d}^3 p|_{-\eta}}{E_h \mathrm{d}^3 \sigma_{pp}^h / \mathrm{d}^3 p|_{-\eta}} \bigg/ \frac{E_h \mathrm{d}^3 \sigma_{dAu}^h / \mathrm{d}^3 p|_\eta}{E_h \mathrm{d}^3 \sigma_{pp}^h / \mathrm{d}^3 p|_\eta} \,. \tag{3.2}$$

As discussed in Ref. [21], the *pp* rapidity distribution is symmetric around $y = 0$ and thus cancels. We therefore obtain:

$$Y_{Asym}^h(p_T) = R_\eta^h(p_T) = \frac{R_{dAu}^h(p_T, -\eta)}{R_{dAu}^h(p_T, \eta)} \,. \tag{3.3}$$

4. Nuclear shadowing and multiple scattering

We expect that particle production in *pA* and *dA* collisions will be different in the forward and backward directions. This is because the respective partons have different momentum fractions (shadowing differences) and because the forward-going parton has to traverse a large amount of matter. In this Section we therefore study the interplay of shadowing and multiple scattering in more detail using the HIJING parameterization.
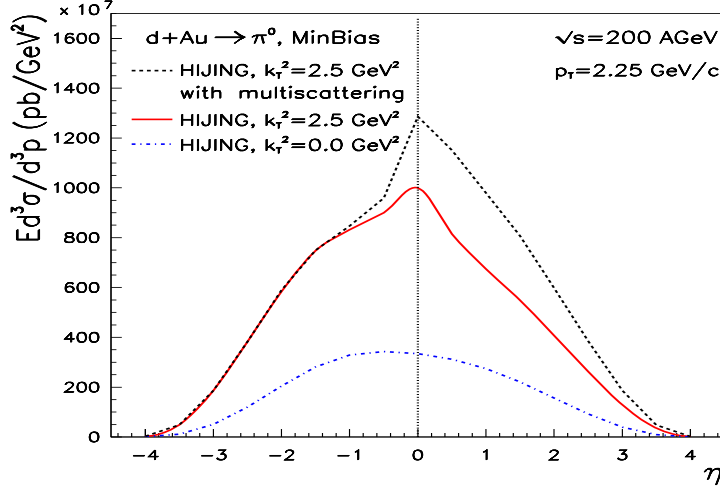

Figure 1: (Color Online) Pseudorapidity distribution for minimum bias neutral pion production from *dAu* collisions at 200 *A*GeV. The solid line represents HIJING shadowing with intrinsic k_T in the proton, the dashed line is HIJING with intrinsic k_T and multiple scattering, while the dot- dashed curve is obtained by turning off any transverse momentum.

In Fig. 1 we display the pseudorapidity distribution for neutral pion production from *dAu* collisions at a fixed p_T (= 2.25 GeV/c). The parameters of eq. (2.3) are unchanged from our previous studies at midrapidity [22, 17], and we have chosen a transverse momentum value comparable to $\langle k_T \rangle_{pp}$, where the various effects are clearly displayed.

The results of our study can be summarised as follows: In the absence of shadowing, the distribution is symmetric around midrapidity. With shadowing only, an asymmetry develops: the yield at a fixed negative pseudorapidty, say $\eta = -2$ (*Au* side or "backward") is higher than at the corresponding positive pseudorapidity ($\eta = 2$, *d* side, or "forward"). The inclusion of the intrinsic transverse momentum in the proton, while increasing the yields on both sides, does not affect the forward/backward symmetry. When multiple scattering is included, the yield shows a stronger increase in the forward direction, leading to Y_{Asym} less than unity. Thus we can say that shadowing suppresses the yield more on the *d* side (forward) relative to a symmetric collision, while the multiple scattering contribution is understandably large in the forward direction.

We have carried out similar studies at higher p_T values. When $k_T \ll p_T$, then k_T effects become naturally smaller. Shadowing effects also become smaller as the antishadowing region is approached. Thus, at $p_T \gtrsim 15$ GeV/c the influence of multiple scattering and intrinsic k_T become

negligible. These phenomena are most important at intermediate p_T values, 2 GeV/c $\lesssim p_T \lesssim$ 8 GeV/c at RHIC. It is interesting to note that a similar transverse-momentum region is sensitive to nuclear effects at lower (e.g. CERN SPS) energies, due to the $\sim \log(\sqrt{s})$ scaling of the Cronin peak [23, 24, 25].

5. Pseudorapidity asymmetry results

5.1 Asymmetry in *pBe* collisions at 30.7 GeV

The pseudorapidity asymmetry for the rapidity interval $0.2 < |\eta| < 0.7$ is shown in the upper panel of Fig. 2 compared with the E706 data [6]. Both EPS08 with k_T and HIJING without multiple scattering give very small asymmetries and the data are also consistent with $Y_{Asym} = 1$ for low p_T. The HIJING parameterization with multiple scattering yields somewhat lower values at all transverse momenta. This is due to multiple scattering moderately increasing the yield on the *p*-side relative to that of the *Be*-side. In view of the rather large error bars, all three sets are in reasonable agreement with the data. The lower panel is our prediction for the interval $1.0 < |\eta| < 1.5$. The
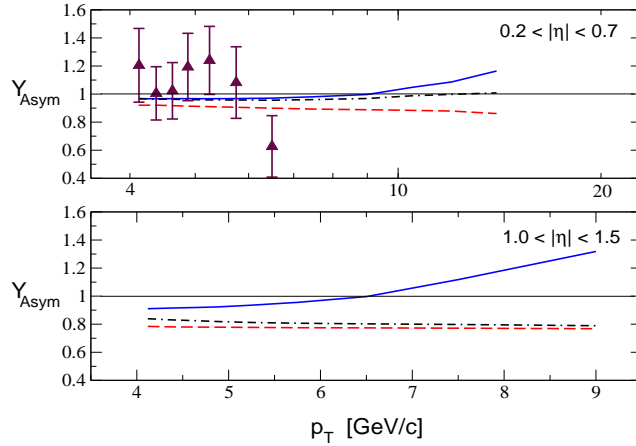

Figure 2: (Color Online) Pseudorapidity asymmetry, Y_{Asym} for $p + Be \rightarrow \pi^0 + X$ at $0.2 < |\eta| < 0.7$ (top) and $1.0 < |\eta| < 1.5$ (bottom). The solid line represents the EPS08 nPDFs, while the dashed line is obtained from HIJING with the inclusion of multiscattering. The dot-dashed line corresponds to HIJING without multiscattering, and filled triangles denote the E706 data [6].

calculated effects here are larger, but with similar structure to those at lower η.

5.2 Asymmetry in *dAu* collisions at 200 *A*GeV

Figure 3 shows the pseudorapidity asymmetry for π^0 production from *dAu* collisions at RHIC, for different pseudorapidity intervals. The two uppermost panels are our results for the asymmetry at $|\eta| < 0.5$ and $0.5 < |\eta| < 1.0$ compared with the STAR data [3]. For $p_T > 4.0$ GeV/c, the agreement with data is quite good for all three sets. At lower p_T, multiple scattering increases the calculated yield mostly in the forward direction as discussed in Sec. 4, leading to calculated
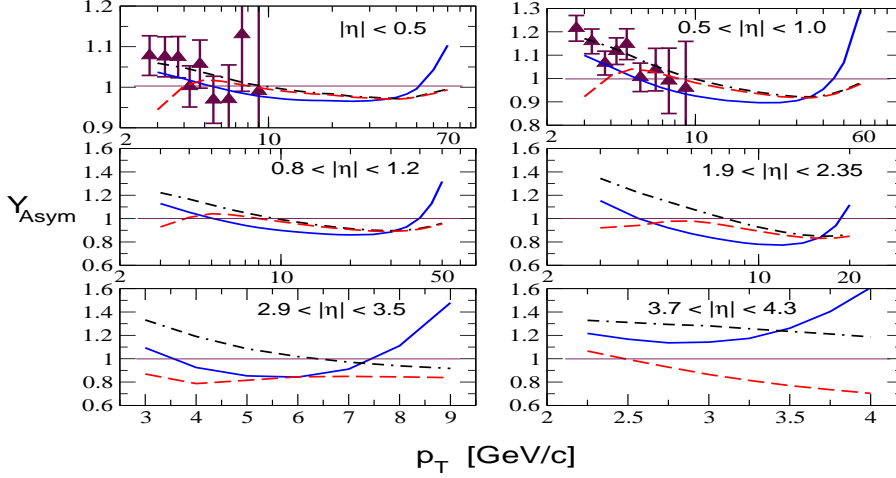
Figure 3: (Color Online) Pseudorapidity asymmetry, Y_{Asym} for $d + Au \to \pi^0 + X$ at different pseudorapidity intervals. The solid line represents the EPS08 nPDFs, while the dashed line is obtained using HIJING shadowing with the inclusion of multiscattering. The dot-dashed line corresponds to HIJING without multiscattering, and filled triangles denote the STAR data [3].

asymmetries below unity. At very high p_T we observe a divergence in the model predictions. The lower four panels are our predictions for the asymmetry as pseudorapidity increases. The first three of these correspond to the BRAHMS pseudorapidity intervals [26]. The general trend is that the asymmetry becomes larger as η increases. This mainly arises from the strong shadowing in the larger nucleus at lower x values. Also, since increasing η leads to decreasing accessible p_T due to phase space constraints, the effects of multiple scattering become more pronounced.

5.3 Asymmetry in *dPb* collisions at 8.8 *A*TeV

Let us now turn to our predictions for the pseudorapidity asymmetry at the LHC energy of 8.8 *A*TeV. The calculated results are displayed in Fig. 4, where the upper panel is for the interval $|\eta| < 0.9$ and the lower panel is for $2.4 < |\eta| < 4.0$. These intervals correspond to acceptance in the central detector and in the muon arm, respectively, of the ALICE experiment [27]. All three sets predict minimal asymmetry of the order of a few percent for the interval $|\eta| < 0.9$. As we move to higher η, the predicted asymmetry becomes more significant. As can be seen in the lower panel of Fig. 4, both EPS08 and HIJING predict substantial asymmetry. According to the model, an LHC measurement of pseudorapidity asymmetry at around $p_T \approx 40$ GeV/c could discriminate between the EPS08 and HIJING shadowing prescriptions.

At the present level, neither model variant gives agreement with all aspects of the data: in an earlier calculation we have found that shadowing parameterizations which do not need to be augmented by a multiple scattering prescription [12, 13, 14] have difficulty describing central-to-peripheral ratios at forward rapidity [15]. We have checked that this also holds for the EPS08 nPDFs. On the other hand, the HIJING parameterization with multiscattering yields pseudorapidity
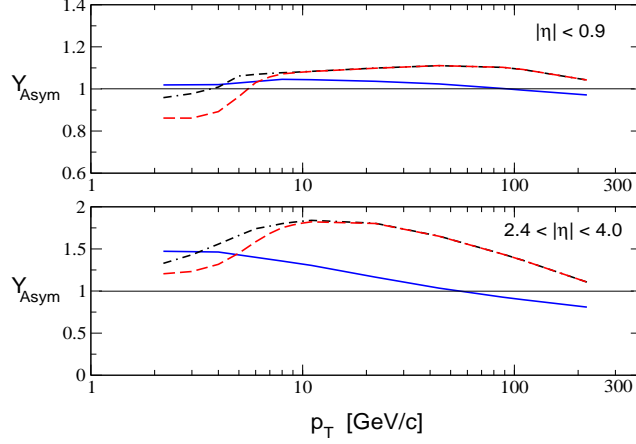
Figure 4: (Color Online) Predicted pseudorapidity asymmetry, Y_{Asym} for $d + Pb \to \pi^0 + X$ at $\sqrt{s} = 8.8$ ATeV for $|\eta| < 0.9$ and $2.4 < |\eta| < 4.0$. The solid line represents the EPS08 nPDFs, while the dashed line is obtained from HIJING with the inclusion of multiscattering. The dot-dashed line corresponds to HIJING without multiscattering.

asymmetries below unity at low transverse momenta.

6. Conclusion

The mechanisms for particle production in asymmetric collisions leads to observable asymmetries in the pseudorapidity distribution of produced particles at some collision energies and transverse momenta. We have considered the effects of nuclear shadowing and multiple scattering on pseudorapidity asymmetry for three asymmetric systems: *pBe*, *dAu*, and *dPb* in a wide c.m. energy range from FERMILAB up to LHC energies.

Overall, the calculated asymmetries are in reasonable agreement with available experimental data. Intrinsic transverse momentum in the nucleon is seen to be important at low p_T. Multiple scattering increases the yield in the "forward" or positive pseudorapidity region, thus leading to a tendency for asymmetries less than unity at low p_T in a scheme explicitly relying on multiple scattering, at variance with the data. An LHC measurement of pseudorapidity asymmetry in *dPb* collisions may be able to distinguish between the EPS08 and HIJING nPDFs at high pseudorapidity and high p_T.

A major constraint in assessing pseudorapidity asymmetries is the limited availability of data for direct comparison with theoretical calculations. More data in asymmetric light-on-heavy collisions separated with respect to positive and negative pseudorapidities are needed to judge calculated pseudorapidity asymmetries. At RHIC, the data from the high-statistic *dAu* Run 8 can be used to provide such a large data sample.

7. Acknowledgments

References

[1] I. Arsene *et al.* [BRAHMS Collaboration], Phys. Rev. Lett. **94**, 032301 (2005).

[2] B. B. Back *et al.* [PHOBOS Collaboration], Phys. Rev. C **72**, 031901 (2005).

[3] B. I. Abelev *et al.* [STAR Collaboration], Phys. Rev. C **76**, 054903 (2007); J. Adams *et al.* [STAR Collaboration], Phys. Rev. C **70**, 064907 (2004).

[4] S. J. Li and X. N. Wang, Phys. Lett. B **527**, 85 (2002).

[5] K. J. Eskola, H. Paukkunen and C. A. Salgado, JHEP **0807**, 102 (2008)

[6] L. Apanasevich *et al.* [Fermilab E706 Collaboration], Phys. Rev. D **68**, 052001 (2003).

[7] S.S. Adler *et al.* [PHENIX Collaboration], Phys. Rev. Lett. **91**, 072303 (2003); Phys. Rev. **C74**, 024904 (2006).

[8] Y. Zhang, G. I. Fai, G. Papp, G. G. Barnafoldi and P. Levai, Phys. Rev. C **65**, 034903 (2002).

[9] J. C. Collins, T. C. Rogers and A. M. Stasto, Phys. Rev. D **77**, 085009 (2008).

[10] M. Czech and A. Szczurek, J. Phys. G **32**, 1253 (2006).

[11] A. D. Martin, R. G. Roberts, W. J. Stirling and R. S. Thorne, Eur. Phys. J. C **23**, 73 (2002).

[12] L. Frankfurt, V. Guzey and M. Strikman, Phys. Rev. D **71**, 054001 (2005).

[13] M. Hirai, S. Kumano and T. H. Nagai, Phys. Rev. C **70**, 044905 (2004); Nucl. Phys. Proc. Suppl. **139**, 21 (2005).

[14] K. J. Eskola, V. J. Kolhinen and C. A. Salgado, Eur. Phys. J. C **9**, 61 (1999).

[15] A. Adeluyi and G. Fai, Phys. Rev. C **76**, 054904 (2007).

[16] S. Albino, B. A. Kniehl and G. Kramer, Nucl. Phys. B **725**, 181 (2005).

[17] P. Levai, G. G. Barnafoldi, G. Fai and G. Papp, Nucl. Phys. A **783**, 101 (2007).

[18] L. Hulthen and M. Sugawara, "Handbuch der Physik", vol. 39 (1957).

[19] D. Kharzeev, E. Levin and M. Nardi, Nucl. Phys. A **730**, 448 (2004)

[20] C. W. De Jager, H. De Vries and C. De Vries, Atom. Data Nucl. Data Tabl. **14**, 479 (1974).

[21] G. G. Barnafoldi, A. Adeluyi, G. Fai, P. Levai and G. Papp, arXiv:0807.3384 [hep-ph].

[22] P. Levai, G. Papp, G. G. Barnafoldi and G. I. Fai, Eur. Phys. J. ST **155**, 89 (2008).

[23] L. Apanasevich *et al.*, Phys. Rev. D **59**, 074007 (1999); L. Apanasevich *et al.* [Fermilab E706 Collaboration], Phys. Rev. Lett. **81**, 2642 (1998).

[24] M. Zielinski, arXiv:hep-ph/9811278.

[25] G. G. Barnafoldi, P. Levai, G. Fai, G. Papp and B. A. Cole, Int. J. Mod. Phys. E **16**, 1923 (2007).

[26] I. Arsene *et al.* [BRAHMS Collaboration], Phys. Rev. Lett. **93**, 242303 (2004).

[27] B. Alessandro *et al.* [ALICE Collaboration], J. Phys. G **32**, 1295 (2006).